ROYAL SOCIETY
OF CHEMISTRY

PAPER

Check for updates

A smart triboelectric nanogenerator with tunable rheological and electrical performance for self-powered multi-sensors†

Sheng Wang, Fang Yuan, Shuai Liu, Jianyu Zhou, Shouhu Xuan, [ID] Yu Wang* and Xinglong Gong [ID] *

A smart magnetorheological elastomer (MRE)-based triboelectric nanogenerator (TENG) with tunable electric–mechanical performance has been developed by assembling MREs, Cu foil and metal wires. The MRE polymer, composed of carbonyl iron and a shear stiffening elastomer matrix, shows a high response to a magnetic field, and the MR effect is 114.68% with a maximum storage modulus of 0.77 MPa. The TENG presents a positive triboelectric performance (PTP) with an increase in the loading pressure. It generates a maximum power of 55.07 μW with a voltage of 20.99 V and lights up 39 LEDs, which proves the high mechanical energy-harvesting properties. More interestingly, the TENG shows a negative triboelectric performance (NTP) under the excitation of a magnetic field owing to the high MR effect and saturated magnetization value of 147.51 emu g^{-1}. Therefore, the overall triboelectric properties of the TENG can be precisely manipulated by alternating the external multi-fields. In addition, the intelligent TENG, with a fast response and high flexibility, functions as a portable self-powered sensor to monitor human motion, distinguish various contact materials, and perceive external magnetic fields. To this end, this work opens up a new avenue to develop a smart TENG device with tunable rheological and triboelectric properties and the self-powered wearable sensor could detect complex multi-field circumstances, which proves it has promising applications in smart energy generation systems and wearable multi-sensing electronics.

Introduction

Smart materials are a kind of composite which can perceive and respond to various external stimuli. The greatest advantages of smart materials are the fast stimuli-responsive effect and the ideal controllability which endows them with wide ranging applications in pneumatic soft robotics,[1] smart windows,[2] catalysis[3] and new power sources.[4] On the other hand, the convertible mechanical, electric and chemical properties of smart materials can be directly manipulated by changing the external excitations. Thus, by recording the alternating properties, smart materials are ideal candidates for use as functional sensors to monitor various working conditions.[5–7]

CAS Key Laboratory of Mechanical Behavior and Design of Materials, Department of Modern Mechanics, CAS Center for Excellence in Complex System Mechanics, University of Science and Technology of China (USTC), Hefei 230027, P. R. China. E-mail: wyu@ustc.edu.cn, gongxl@ustc.edu.cn

† Electronic supplementary information (ESI) available: Movie S1 shows the reported TENG device can gather mechanical energy and light up LED arrays. Movie S2 proves that the TENG on a finger can act as a wearable sensor to detect gentle touch. Movie S3 shows that the light intensity of the LEDs is dramatically decreased (negative triboelectric performance) if a magnetic field is loaded onto the TENG. Movie S4 shows that the TENG acts as a portable bi-mode sensor to monitor human motions and the surrounding magnetic field. See DOI: 10.1039/c9tc05969e

Recently, wearable intelligent sensor devices have become a hot research topic owing to their advantages such as flexibility, their light weight making them comfortable to wear, and their important applications.[8–10] So far, various functional polymers have been applied in intelligent sensors and stretchable electronics, enabling mechanical stimuli to be transduced into electrical signals, which are desirable in human–machine interactions, electrical engineering areas and medical diagnoses.[11–13] However, sensors are often used in sophisticated environments in which various electromagnetic waves exist, particularly during the operation and opening of machines. Therefore, further efforts should be made to develop functional sensors to distinguish different stimuli in complex multi-field circumstances.

A magnetorheological elastomer (MRE) is a kind of stimuli-responsive composite for which the magnetorheological (MR) properties can be adjusted rapidly and reversibly by a magnetic field.[14,15] Thus, many functional materials based on smart magnetorheological elastomers (MREs) have also been developed and their mechanical and electrical properties show favorable tunability.[16] In particular, smart magnetoresistive composites with a magnetic–electric coupling effect, are a type of material in which the conductivity demonstrates magnetic field dependent characteristics.[17] Thus, they are favorable for use as pressure,

biomedicine and magnetic field sensors.[18–20] An intelligent magnetorheological composite with controllable conductivity was developed and a particle–particle resistance model was proposed to investigate the magnetic field dependent electroconductivity.[21] A novel conductive MRE sponge with high flexibility and large deformation was prepared and the mechanic–electric–magnetic coupling properties under various stimuli were systematically explored.[22] Moreover, a functional magnetic-conductive MRE fiber was also successfully constructed and the gripper showed a high potential for magnetic field sensors.[23] Very recently, a novel liquid metal-based MRE with positive piezoconductivity has been developed.[24] In addition to sensing various external pressures, it also showed magnetic field-responsive thermal properties. However, rigid batteries are required as external power sources to actuate these electronic sensor devices. The disadvantages of the bulk volume, limited lifespan and potential environmental hazards of batteries also restrict the large-scale use of these smart sensors. The instability of the surface adhesion between the MRE matrix and the two electrodes also causes inaccuracy in the sensing results. A mainstream tendency of wearable system is endowing smart electronics with self-powered characteristics as they are more practical, favorable and show greater potential application prospects in the future. Thus, developing novel self-powered multifunctional sensors to monitor various stimuli including magnetic fields still remains a challenge.

A triboelectric nanogenerator (TENG), a device which could scavenge mechanical energy and transform it into electrical energy, can act as a promising renewable energy generation system owing to the coupling effect of triboelectrification and electrostatic induction.[25] Owing to the widespread kinetic energy, ideal flexibility and high output electrical properties, triboelectric nanogenerators (TENGs) have been successfully utilized as novel power sources for wearable electronics, as well as self-powered sensors, to explore external excitations such as pressures, human motions and wind.[26–29] Recently, novel TENG systems with energy-harvesting and storage properties have also been generated.[30] Although the developed TENGs could harvest various irregular mechanical impulses, the output triboelectric performance is influenced by the loading kinetic energy. However, smart TENGs with the controllable mechanic–electric coupling properties have seldom been reported. In addition, although several works have been devoted to designing self-powered nanogenerators based on the coupling of TENGs and electromagnetic generators for monitoring ambient magnetic fields,[31,32] the hybrid TENGs with stiff coils, metal springs, a magnet and complicated structures were bulky. They could not be worn which hindered their practical applications in flexible electronics. The properties of these TENGs could also not be directly manipulated. Shear stiffening gel (SSG), a derivative of polyborosiloxane, is a smart polymer with controllable storage modulus which can be used in damping and vibration control. It is soft and viscoelastic at room temperature, showing the high stretchability. Its surface is sticky and this good adhesion is beneficial for assembling smart devices. Furthermore, the SSG-based MR materials have also been proven to have high magneto-responsive properties.[16] In this regard, introducing a

smart shear stiffening material-based MRE into nano-generators may provide a novel and easy strategy to develop novel functional intelligent TENGs with controllable mechanical–electrical property and the self-powered wearable sensor based on these may be able to detect external multi-fields.

In this work, a wearable intelligent TENG based on MRE has been developed. The MRE was fabricated by introducing carbonyl iron (CI) particles into SSG/PDMS (shear stiffening gel/polydimethylsiloxane, referred to as the shear stiffening elastomer (SSE)) and the rheological properties of MRE show a fast response to the magnetic field, for which the MR effect is 114.68%. The TENG device can effectively harvest mechanical energy and the maximum output power is 55.07 μW. More importantly, the loading pressure and magnetic field demonstrate a positive and negative influence, respectively, on the triboelectric performance of TENG which indicates the electrical properties can be directly manipulated by external fields and mechanical force. In addition, the portable TENG device has been proven as a self-powered sensor to distinguish various excitations including human movements and magnetic fields. The reason for this is that the increased storage modulus and stiffness under the magnetic field leads to small compression deformations and contact areas which further depresses the electron transformation and finally results in negative triboelectric effects.

Results and discussion

Preparation and characterization of the TENG

The fabrication procedures for the TENG are presented in Fig. 1. As SSG is soft and plastic, its creep behavior is apparent and a small amount of silicone rubber was first introduced into the SSG by a two roll miller to improve the mechanical properties and stability.[33] Then, the curing agents were added. The mixture material is referred to as the SSE. During the mixing process, various mass fractions of CI particles were also mixed. Finally, the above compounds were vulcanized. Fig. 1a shows the tailored cured SSE-60% cylinder with a diameter and thickness of 20 × 1 mm, together with the Cu film and a conductive wire they were assembled into TENGs (Fig. 1b–d). Derived from SSG, two pieces of the prepared stretchable SSEs with a stable configuration can adhere to each other after they come into contact (Fig. 1f and g).[33,34] Thus, the SSE polymer is an ideal candidate matrix for the easy-to-manufacture flexible TENGs.

Microstructures of the composites were also studied. The SEM image in Fig. 1h exhibits the particle diameter of CI is about 3 μm. Micro-wrinkles appear on the surface of SSE which indicates its soft characteristics (Fig. 1i). Several CI agglomerations can be observed on the SSE-20% (Fig. 1j) and more CI particles exist if the mass fraction increases to 60% (Fig. 1k and l). It has been proven that the CI particles can move in the direction of the external magnetic field which forms particle chains.[35] Fig. 1f also shows the CI particle chains formed if SSE-60% are subjected to a 200 mT magnetic field for a long time. This phenomenon proves the micro-structure, as well as the rheological properties, of the as-prepared material can be manipulated by a magnetic field.
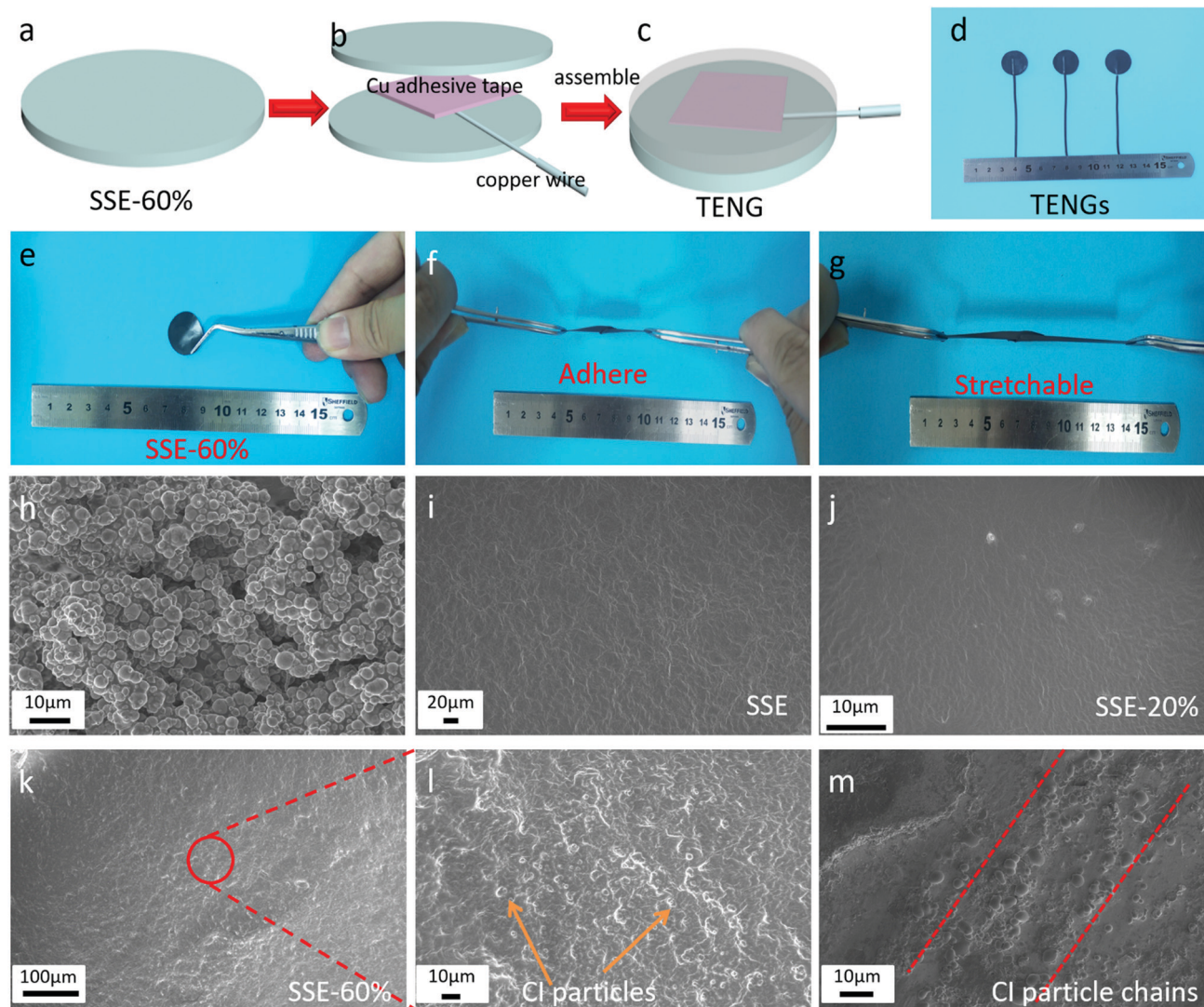
3716 | J. Mater. Chem. C, 2020, 8, 3715–3723

This journal is © The Royal Society of Chemistry 2020

Fig. 1 Preparation procedures of the SSE-based TENG: (a) pristine SSE-60%; (b) and (c) assembling SSE-60%, Cu conductive adhesive tape and copper wire together and then covering with the other SSE-60% to form a TENG device; (d) the as-prepared TENGs; (e) the shape of SSE-60% and the sticky surface; and (f) and (g) when the two pieces of SSE-60% come into contact, they can adhere and be stretched without breakage. SEM images of: (h) CI spherical particles; and (i) the surface of pure SSE, which is wrinkled. (j) Particles could be observed on SSE-20%; and (k) and (l) SSE-60%. (m) The CI particles are rearranged to form chains with the excitation of the magnetic field.

The rheological properties of the as-prepared polymer composites were studied using a commercial rheometer. The storage modulus (G') of all polymer composites increased with the increase in the shear frequency and CI content, which also enhanced the mechanical properties (Fig. 2a). It has been proven that the SSG-CI magnetorheological gel possesses a high MR effect.[16] Thus, the magnetic field dependent rheological performance of SSE-CI was also studied (Fig. 2c). Undoubtedly, the G' of all magnetorheological materials is proportional to the magnetic flux density which exhibits a remarkable MR effect. For example, the initial G' of MRE-40% is 0.25 MPa and it reached 0.35 MPa at a magnetic field of 1200 mT. The MR effect is 40%. The CI contents also showed a positive influence on the MR properties which indicates that a higher CI content induces a larger MR effect. The maximum G' of MRE-60% was 0.77 MPa and the

relative MR effect was 114.68%. However, MRE-0% (no CI particles) exhibits no magnetic field dependency and the initial and final G' values were 0.12 and 0.13 MPa, respectively. The remarkable MR effects are due to the high intrinsic magnetization of the CI particles (Fig. 2b). All of the composites exhibit typical soft magnetic behavior and the saturated magnetization values of MRE-20%, MRE-40%, MRE-60% and CI particles were 52.68, 99.95, 147.51 and 206.77 emu g^{-1} respectively. As for MRE-0%, the G' is independent of the magnetic field and the magnetization is maintained at 0.83 emu g^{-1} in the range of 0–1200 mT. The responsive effects of MRE-60% under different step magnetic fields are presented in Fig. 2d. The storage modulus remains at about 0.35 MPa in the absence of a magnetic field and it increases sharply once a step magnetic field of 120 mT is applied and is gradually saturated at 0.45 MPa. After removing

This journal is © The Royal Society of Chemistry 2020

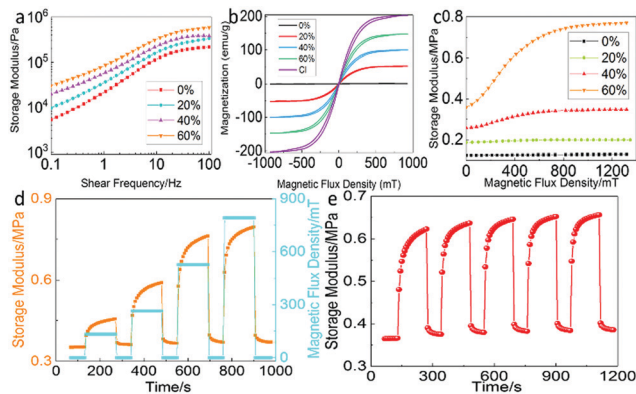*J. Mater. Chem. C*, 2020, **8**, 3715–3723 | **3717**

Fig. 2 (a) Storage modulus values of the as-prepared polymers at different shear frequencies; (b) the magnetic hysteresis loops; and (c) magnetic field dependent modulus values of the composites with different CI content values. (d) The response effects of the as-prepared SSE-60% to different magnetic fields and (e) the cyclic stability under the excitation of a magnetic field.

the fields, the modulus drops dramatically to the initial values. Undoubtedly, the enhanced rheological properties of MRE-60% are also proportional to the step magnetic fields at which the G' changes to 0.79 MPa when the external magnetic field is 792 mT. The G' also shows an ideal stability under cyclic loading–unloading excitation with 340 mT (Fig. 2e). Thus, the reported MRE-60% with controllable mechanical properties and a fast response to a magnetic field shows promise for application in the development of smart TENGs.

Triboelectric performance of the TENG

The TENG has been proven to be an effective device in harvesting and converting kinetic energy into electrical energy.[36] Thus, the reported TENG also gathers energy and successfully lights up 39

LEDs (Fig. 3a and Movie S1, ESI†). The load resistance dependent triboelectric performance of the device was also investigated (Table S1, ESI†). The voltage (blue line in Fig. 3c) of the TENG was as low as 0.01 V at a resistance of 1 kΩ and it showed a dramatic increase when the resistance was larger than 100 kΩ and finally reached 38.57 V under 1 GΩ. However, when the maximum current was 12.29 μA (at 1 kΩ), it showed a decreasing tendency and finally reached as low as 0.04 μA (at 1 GΩ). The relationship between the output power and load resistance is calculated in Fig. 2d. The instantaneous power first increases with the increase in the resistance and after achieving the maximum value, it starts to decrease. The maximum power of the as-prepared TENG under compression force is as high as 55.07 μW at the resistance of 8 MΩ with a voltage of 20.99 V. The current also shows stability under cyclic loading–unloading excitations (Fig. 2b). To this end, a MRE-based TENG with highly efficient energy-harvesting properties has been constructed.

In consideration of the high flexibility, energy-collecting effects and good sensitivity, the as-designed TENG could be worn on the hand (Fig. 4a). During walking, the fingers touch the clothes and the TENG sensor can feel this contact process by changing the output voltages from 0.14 to 0.27 V (Fig. 4b) which acts as a wearable self-powered artificial electronic skin device. To mimic the recognition performance of TENG, materials with varying friction including Al foil, Cu plate, nitrile, silk fiber, PC plate, glass, PDMS, apple and polytetrafluoroethylene (PTFE) film have been applied to rub on the TENG. Owing to the variable triboelectrification, the TENG outputs different voltages when it comes into contact with various materials (Fig. 4c). For example, the peak voltage is 15.52 V when touches an Al film and it decreases to 9.59 V when rubbed on a silk layer. Fig. 4d presents the perception results of the TENG. The voltage is apparently higher when pressed onto Al foil and nitrile, similar results have also been reported previously.[37] When in contact with a PTFE film, a negative voltage of −5.90 V is observed, which is due to the high electron capturing characteristics of PTFE. These results
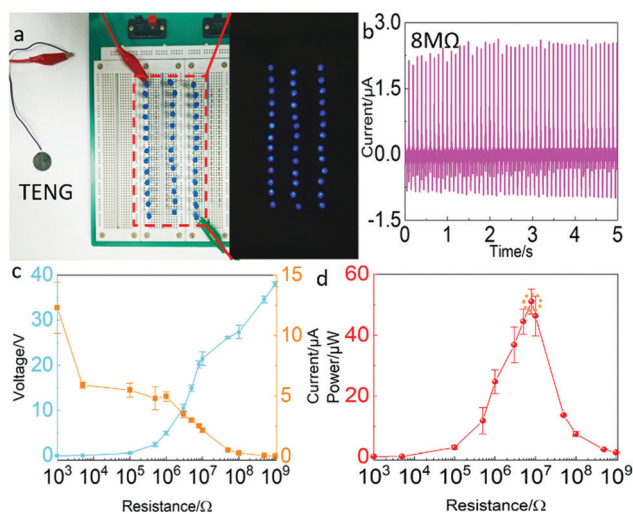

Fig. 3 (a) The TENG can collect and transform mechanical energy into electric energy and light up LED arrays. (b) Typical curves for the voltage under 8 MΩ, and the triboelectric performance, including (c) the current, voltage and (d) output power at a loading force and frequency of 60 N and 10 Hz under various external resistance values.
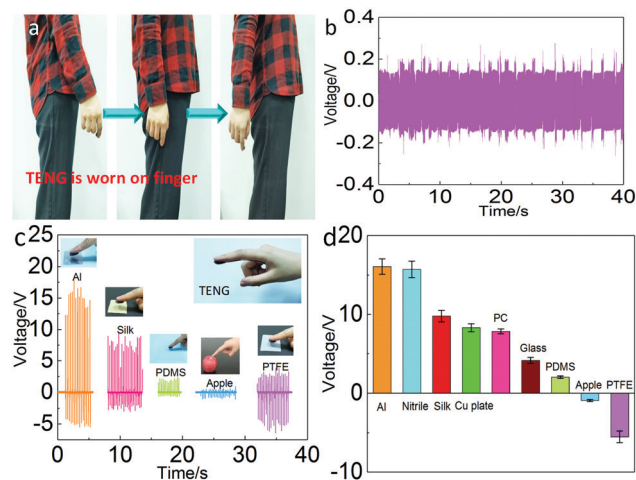

Fig. 4 The TENG works as a wearable self-powered sensor to (a and b) monitor walking in humans and (c and d) distinguish between different contact materials (including metals, polymers, fibers and inorganic materials).
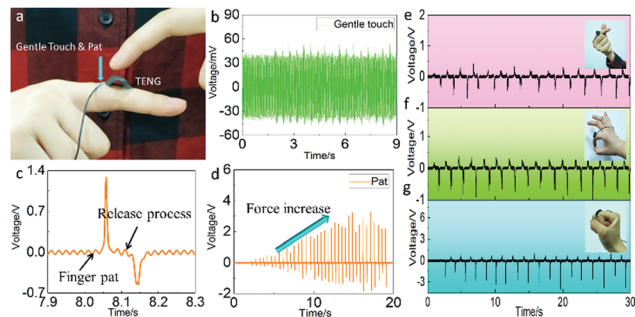
Fig. 5 Wearable TENG finger monitors: (a and b) gentle touch and (d) increasing the compressive force, (c) voltage variation in one pat-release process, and (e–g) the physiological motion sensing behaviors of the TENG from various finger gestures.

demonstrate that the electrical properties of the TENG can be significantly influenced by the friction layer materials and the variation in the voltages could be used to assess contact with different materials, which implies potential applications in tactile perception sensors.

Fig. 5 further displays the application of this self-powered TENG as a proof-of-concept foldable and wearable sensor. The TENG device can be bent and mounted on fingers (Fig. 5a and Movie S2, ESI†). With a high sensitivity, it can distinguish a gentle touch by immediately outputting voltages from 43 to 55 mV (Fig. 5b) and it also shows stability under cyclic touch stimuli. Fig. 5c exhibits the voltage variation in one pat-release process and the voltage increases within 43 ms, indicating the fast response properties of the TENG. The voltages increase dramatically with the increase in the compression forces and are finally maintained at 2.60 V when the loading force is constant (Fig. 5d). The force-dependent characteristics of the voltage signals can also be used to assess external violent compressions. In addition, various human finger gestures were also monitored and distinguished using the TENG (Fig. 5e–g). From Fig. 5e it can be seen that the voltage signals possess sharper and larger peak values in the downward direction and lower peak values in the upward direction. The negative voltages decrease with the increase in finger bending. A value of -0.73 V was observed when a "OK" gesture was made, which varied to -2.90 V if a clenched hand gesture was made. In conclusion, the as-designed TENG with a high sensitivity, fast response, self-powered tactile-perception behavior and cyclic reliability has been proven to have potential applications for monitoring and analyzing human motions.

Magnetic field dependent electrical properties of the TENG

Owing to the tunable MR effect, a homemade experimental setup was used to systematically investigate the magnetic field responsive triboelectric performance (Fig. 6a and b). The TENG device is adhered on a polycarbonate (PC) plate and a magnet is placed below it. During the tests, finger compression is continuously loaded onto the TENG and it can harvest mechanical energy and light up LEDs (Fig. 6c). However, the light intensity is dramatically decreased once a magnet is next to the TENG

which implies that the magnetic field can remarkably influence the electrical properties of the device (Fig. 6d and Movie S3, ESI†). Under the gentle touch of a finger, the output voltage is about 1.1 V, but it decreases to 0.6 V once subjected to a magnetic field and the signal recovers as the magnet moves quickly through the TENG (Fig. 6e). The passing route of the magnet is presented in Fig. S1 (ESI†). Similarly, the voltage curves show a decreasing trend if the magnet passes slowly through the TENG, as it is still simultaneously compressed intensely by a human finger (Fig. S2, ESI†).

Therefore, to further evaluate the synergistic influence of the loading force and magnetic field on the electrical properties of the TENG, a characterization system, as presented in Fig. 6g, was applied. The schematic diagram shows that the TENG device is attached to a PC plate and it is mechanically triggered by an oscillator. During tests, the magnetic flux density around the TENG was adjusted by changing the distance between the magnet and the TENG (using PC plates with different thicknesses) and the magnetic field values were measured using a tesla meter. The distribution simulation of the magnetic induction lines for the magnet is also presented in Fig. 6f. Clearly, the magnetic strength declined with the increase in the distance. During the tests, an 8 MΩ resistor was connected in the circuit. When the magnetic field was 0 mT, the TENG showed a high sensitivity and a voltage of 3.43 V was outputted if the compression force was 0.7 N, which proves that it can even harvest and sense slight mechanical triggers (Fig. S3a and Table S2, ESI†). The voltages were undoubtedly increased to 20.98 V once the loading force changed to 60 N. However, the triboelectric performance decreased once a magnetic field was applied to the TENG. For example, the maximum voltage decreases to 11.10 V if the surrounding magnetic field is 100 mT (compression force remains at 60 N) (Fig. S3b and Table S3, ESI†). Thus, the output voltages of the TENG device under multi-fields of magnetic flux density and loading forces were further systematically explored and the results are depicted in Fig. 6h. Clearly, the compression forces can dramatically enhance the output voltages of the TENG which exhibits a positive triboelectric performance (PTP). However, the TENG exhibits a negative triboelectric performance (NTP) under magnetic field excitation. Once the magnetic fields increase from 45 to 100 mT, the voltages decrease from 17.13 to 11.10 V (maintaining the force at 60 N). At a magnetic field of 190 mT, the voltages vary from 1.20 to 1.81 V as the loading forces alternate from 10 to 60 N (Table S3, ESI†). This is mainly because the stiffness of SSE-60% increases once a magnetic field is loaded, which leads to decreased deformation and a small contact area under the excitation of the compression forces. Apparently, the magnetic field shows a negative enhancement in the triboelectric effect. Based on the PTP and NTP effects, we can conclude that the triboelectric performance of the as-prepared smart TENG could be directionally regulated by controlling the external magnetic fields and compression forces and the output voltages can be varied in large areas.

On the other hand, the results of the voltage–loading forces under different magnetic fields and the voltage–magnetic flux
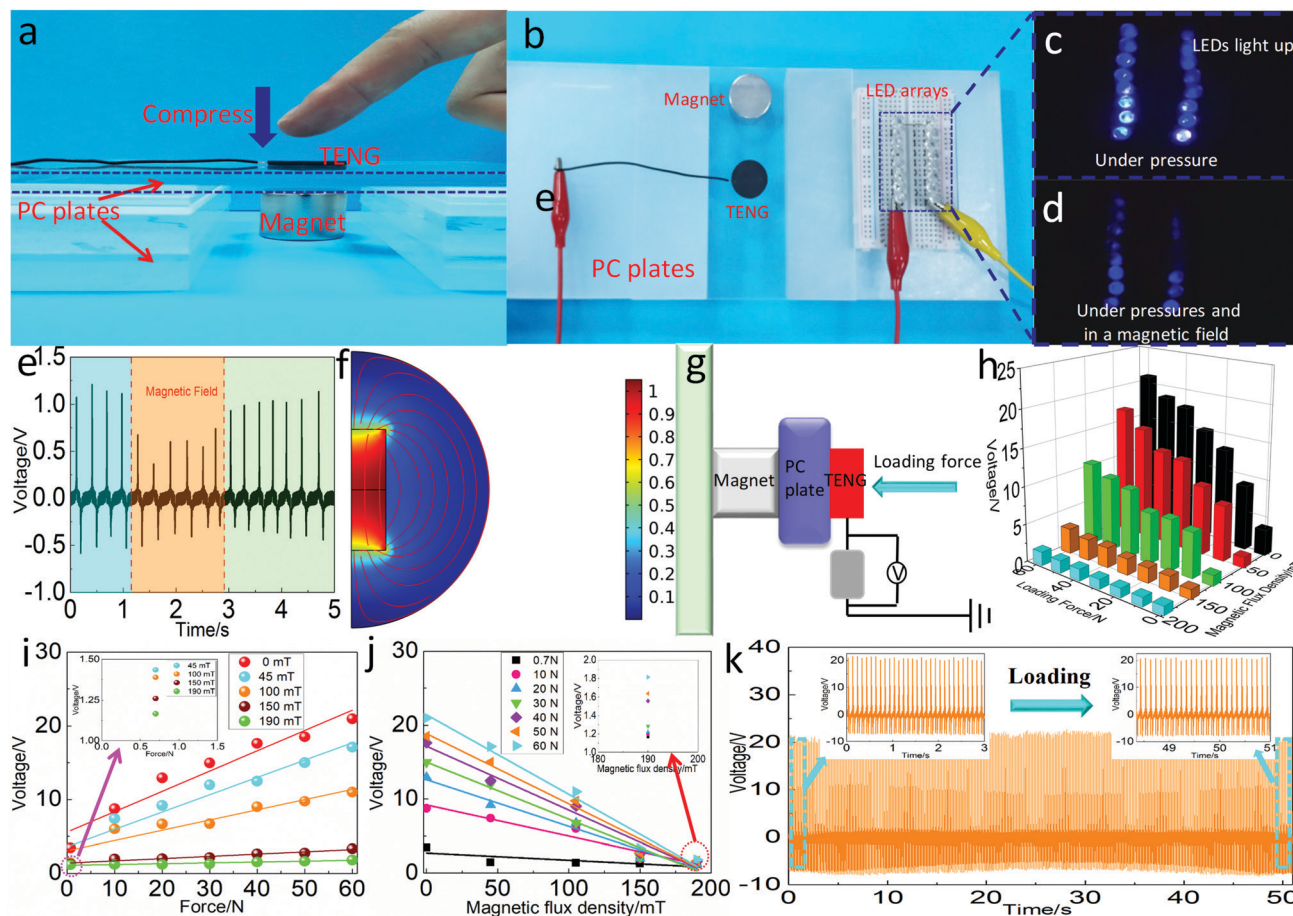
This journal is © The Royal Society of Chemistry 2020

J. Mater. Chem. C, 2020, **8**, 3715–3723 | **3719**

Fig. 6 (a) A photo showing the experimental system for assessing the influence of the magnetic field on TENG performance, (b) the top view of the system, (c) the TENG lights up LEDs, (d) the light intensity is decreased under excitation from a magnet, (e) the voltage responds to magnetic fields when a magnet passes over the TENG, and (f) the magnetic simulation result for a magnet. (g) A schematic illustration of the triboelectric test system for harvesting mechanical energy with a magnet, polycarbonate plate and the TENG, (h) the force and magnetic field dependent triboelectric performance of TENG, the experimental and fitting curves of: (i) voltage–loading forces under different magnetic fields; and (j) voltage–magnetic flux density under different compression forces. (k) The recovery properties and cyclic stability of the TENG after unloading the magnetic field.

density under different compressive forces were also fitted. From Fig. 6i, the TENG exhibits different force sensitivities when the device works at various magnetic fields. The output voltages increase almost linearly with the increasing pressures and the slopes of all of the fitted curves represent the sensitivity to loading forces. For example, the sensitivity is 0.030 V N^{-1} under 150 mT, and this changes to 0.24 V N^{-1} under 45 mT. Furthermore, the magnetic field shows a negative influence on the voltages when maintaining a constant loading pressure (Fig. 6j). According to the results, the magnetic sensitivities under different pressures are also regarded as linear which is favorable for practical industrial applications. Similarly, the sensitivities of TENG are −0.0097, −0.042, −0.063, −0.077, −0.081, −0.095 and −0.011 V mT^{-1} in the range of 0.7–60 N. Owing to the good flexibility and high sensitivity, this wearable TENG can act as a self-powered force sensor and the external forces and magnetic field can also be assessed using linear equations from Fig. 6i and j. As for the pure SSE (no CI particles)-based TENG, the triboelectric performance undoubtedly shows no magnetic field dependent effects, for which the

maximum voltages under 0 and 180 mT are 19.31 and 18.93 V respectively (Fig. S4, ESI†).

The recovery performance and cyclic stability of the TENG after removal of the magnetic fields were also explored in Fig. 6k. Clearly, the voltage can recover to 20.33 V which presents a degradation of 3.14% (before loading the magnetic field, the voltage is 20.99 V once the compression force was maintained at 60 N). The voltage signals also show excellent stability even after 500 compression-release excitations owing to the ideal durability of the SSE polymer matrix. To this end, the as-designed wearable TENG device with functional stimuli-responsive properties is more desirable as a smart power source and multifunctional bi-mode sensor for actuating low-power electronic devices and sensing complex multi-fields in practical working conditions.

Taking advantage of the good sensitivity to multiple stimuli and the high flexibility, the TENG can act as a proof-of-concept self-powered bi-mode sensor for physiological motions and the surrounding magnetic fields. The finger bends to different degrees (Fig. 7a–d) and the wearable TENG can perceive the bending-releasing behaviors by changing the voltages from approximately
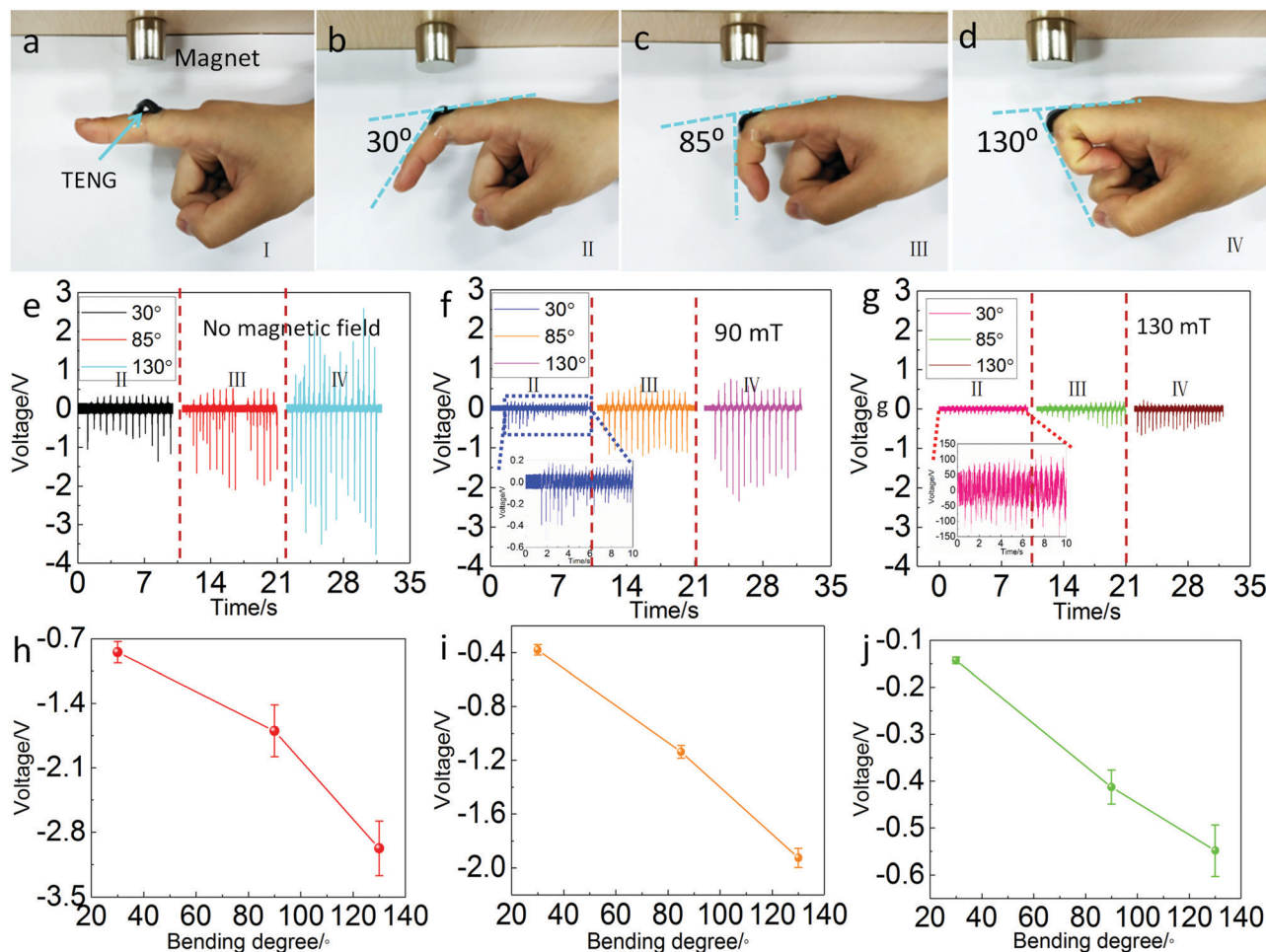
Fig. 7 (a–d) The TENG acts as a portable bi-mode sensor to monitor human motion and the surrounding magnetic fields: photographs of finger bending with different degrees, and the self-powered sensing of the TENG under magnetic fields of: (e) 0; (f) 90; and (g) 130 mT. (h–j) The corresponding respective maximum voltages with error bars.

−0.85 to −2.98 V with an increase of 30–130° (Fig. 7e and h). Interestingly, the output voltages are dramatically increased under the excitation of magnetic fields (Fig. 7f, g and Movie S4, ESI†). For example, the TENG could still feel the bending motions under the magnetic field of 130 mT from the voltages of about −0.14 V with a 30 degree bending stimuli and the average voltages changed from −1.93 to −0.55 V when the magnetic field increased from 90 to 130 mT under a bending degree of 130° (Fig. 7i and j). On the other hand, if the output voltage signals vary from −2.98 to −0.55 V under a 130° bending, it indicates that the surrounding magnetic flux density is about 130 mT. In conclusion, the easy-to-manufacture wearable TENG based on the MR SSE matrix monitors various physiological motions and it also shows a high reliability for assessing external magnetic fields by finger bending motions only, which is more convenient for practical applications.

Working mechanism of the smart TENG

The working mechanism of the TENG is mainly dependent on the coupling effect of the triboelectrification and the electrostatic induction. SSE is very soft and the surface of the TENG

device is rough (Fig. 8a). Thus, the raised SSE matrixes are compressed and the deformation of TENG is apparently large under the loading of an external force, which leads to total contact between the human hand and the TENG. Therefore, large numbers of electrons transfer from the fingers to the surface of the TENG owing to their different electron affinities (Fig. 8b). As the fingers leave, residual negative charges on SSE will induce positive charges on the electrode. On this occasion, the positive charges could drive the free electrons to flow from the Cu tape to the ground which generates higher output current signals (Fig. 8c). However, the mass amount of CI particles dispersed in the MR polymer matrix could reduce the electronegativity of the TENG which further impedes the electron transformation from the human skin to the MR elastomer surface (Fig. 8d). On the other hand, the storage modulus and stiffness of the smart TENG significantly increases under the excitation of a magnetic field. Therefore, the compressive deformation is smaller compared with the SSE-based TENG during the loading-unloading process (Fig. 8e). The raised SSE/CI matrixes are difficult to compress and larger spaces between the human hand and the TENG surface diminish the contact areas,
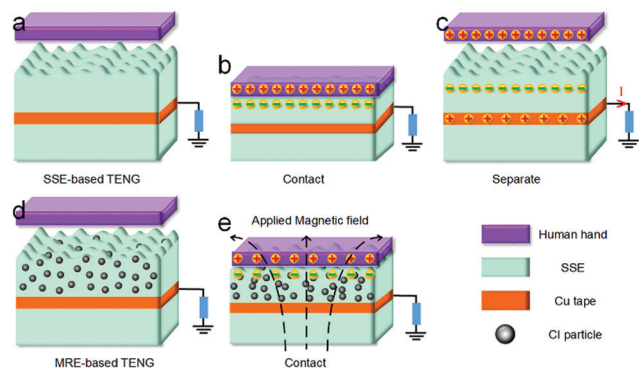
This journal is © The Royal Society of Chemistry 2020

J. Mater. Chem. C, 2020, **8**, 3715–3723 | **3721**

Fig. 8 Working mechanism of the TENG: (a) pristine, (b) and (c) current generating process of the SSE-based TENG, (d) MRE-based TENG and (e) the device under the excitation of a magnetic field and compression force.

leading to reduced electron transformation. Owing to the reversible rheological properties of the MR elastomer, the storage modulus decreases to the initial values once the magnetic field is unloaded. Therefore, the triboelectric properties also vary in the pristine state. In conclusion, the as-designed smart TENG shows a force and magneto controllable triboelectric performance in large areas which could act as a wearable sensor to distinguish between different stimuli in complex multi-field working conditions.

Experimental section

Preparation of the TENG

The preparation procedure for SSG was reported in our previous work.[16] Briefly, a mixed composite composed of PDMS, pyroboric acid (heated by boric acid) and a small amount of alcohol was polymerized at 240 °C to obtain a solid SSG material. After cooling down, SSG and PDMS with a mass ratio of 7:3 were mixed using a two-roller miller and referred to as SSE. During the preparation process, benzoyl peroxide and different amounts of the CI particles were added to prepare the magnetorheological material (named SSE-X, in which X indicates the mass of CI particles). Then, the composites were placed in steel molds and cured using a plate vulcanizer (Model: BL-6170-B) at 100 °C and 20 MPa for 15 min. The triboelectric nanogenerator was fabricated by assembling two pieces of the as-prepared MR elastomers with a diameter of 20 mm and a thickness of 1 mm, Cu conductive adhesive tape and copper wires and followed by compression for 1 min.

Characterization systems

The microstructures of all composites were observed using SEM (Gemini SEM 500, ZEISS). The rheological properties were characterized using a commercial rheometer (Physica MCR 301, Anton Paar Co., Austria). Samples were molded into cylinders with a thickness and diameter of 1 and 20 mm, respectively. The triboelectric properties were recorded using a digital multi-meter (DMM6001) and the compression force was loaded using an oscillator (HEV 500). The magnetic field was loaded using a commercial cylindrical magnet with a diameter and height of

20×25 mm and the magnetic flux density loaded on TENG was measured using a tesla meter (HT20). The magnetic hysteresis loops were investigated using a hysteresis measurement of soft and hard magnetic materials (HyMDC Metis, Leuven, Belgium).

Conclusions

In this work, a smart triboelectric nanogenerator with controllable triboelectric performance and multifunctional sensing effects has been designed by assembling Cu foil with a magnetorheological SSE elastomer. The as-prepared SSE-60% shows a high MR effect of 114.68% and the maximum storage modulus is 0.77 MPa. The TENG, with a thickness of 4 mm, demonstrates a high efficiency in harvesting mechanical energy with a current of 2.62 μA, and a maximum output power of 55.07 μW, which can light up 39 LEDs. Undoubtedly, the output voltage is proportional to the compression force. More importantly, the triboelectric properties of the TENG could be directly controlled by the external magnetic field. The voltage decreases from 20.99 to 1.81 V if the external magnetic flux density is increased from 0 to 190 mT (maintaining the compression force at 60 N). Acting as a self-powered sensor, the nano-generator also shows multiple sensing performances and can assess various physiological movements, such as gentle touching, compression, and finger bending. The high saturated magnetization values also prove that the TENG can be used as a functional sensor to assess the external magnetic field. Thus, the MR-based TENG with reliable multi-functions has the potential for practical utilization in wearable electronics, green energy sources and multi-field sensing areas.

Conflicts of interest

There are no conflicts to declare.

Acknowledgements

References

1 E. Siéfert, E. Reyssat and J. B. B. Roman, *Nat. Mater.*, 2019, **18**, 24–28.
2 T. D. Vu, Z. Chen, X. T. Zeng, M. Jiang, S. Y. Liu, Y. F. Gao and Y. Long, *J. Mater. Chem. C*, 2019, 7, 2121–2145.

3722 | *J. Mater. Chem. C*, 2020, **8**, 3715–3723

This journal is © The Royal Society of Chemistry 2020

3 C. Han, M. Y. Qi, Z. R. Tang, J. L. Gong and Y. J. Xu, *Nano Today*, 2019, **27**, 48–72.

4 A. Chandrasekhar, N. R. Alluri, V. Vivekananthan, Y. Purusothaman and S. J. Kim, *J. Mater. Chem. C*, 2017, **5**, 1488–1493.

5 J. M. Habertl, F. A. Sanchez, A. M. Mihut, H. Dietsch, A. M. Hirt and R. Zezzenga, *Adv. Mater.*, 2013, **25**, 1787–1791.

6 X. S. Zhang, J. Brugger and B. Kim, *Nano Energy*, 2016, **20**, 37–47.

7 R. Zhang, Q. Wang and X. Zheng, *J. Mater. Chem. C*, 2018, **6**, 3182–3199.

8 Y. H. Jia, L. L. Shen, J. Liu, W. Q. Zhou, Y. K. Du, J. K. Xu, C. C. Liu, G. Zhang, Z. S. Zhang and F. X. Jiang, *J. Mater. Chem. C*, 2019, **7**, 3496–3502.

9 Y. J. Lu, M. W. Tian, X. T. Sun, N. Pan, F. X. Chen, S. F. Zhu, X. S. Zhang and S. J. Chen, *Composites, Part A*, 2019, **117**, 202–210.

10 X. X. Kong, J. Li, W. Collins, C. Bennett, S. Laflamme and H. Jo, *Smart Mater. Struct.*, 2018, **27**, 115008.

11 M. Amjadi, K. U. Kyung, I. Park and M. Sitti, *Adv. Funct. Mater.*, 2016, **26**, 1678–1698.

12 J. Wen, Y. Tian, C. Hao, S. Wang, Z. Mei, W. Wu, J. Lu, Z. Zheng and Y. Tian, *J. Mater. Chem. C*, 2019, **7**, 1188–1198.

13 Y. J. Zheng, Y. L. Li, K. Dai, M. R. Liu, K. K. Zhou, G. Q. Zheng, C. T. Liu and C. Y. Shen, *Composites, Part A*, 2017, **101**, 41–49.

14 H. M. Pang, L. Pei, C. L. Sun and X. L. Gong, *J. Rheol.*, 2019, **62**, 1409–1418.

15 M. Yu, S. Qi, J. Fu and M. Zhu, *Appl. Phys. Lett.*, 2015, **107**, 111901.

16 S. Wang, W. Q. Jiang, W. F. Jiang, F. Ye, Y. Mao, S. H. Xuan and X. L. Gong, *J. Mater. Chem. C*, 2014, **2**(34), 7133–7140.

17 T. Kobayashi, T. Matsishita, T. Mizushima, A. Tsuruta and S. Fujimoto, *Phys. Rev. Lett.*, 2018, **121**, 207002.

18 I. Giouroudi and E. Hristoforou, *J. Appl. Phys.*, 2018, **124**, 030902.

19 X. Zhang, N. Vernier, Z. Cao, Q. Leng, A. Cao, D. Ravelosona and W. Zhao, *Nanotechnology*, 2018, **29**, 365502.

20 L. Ge, X. Gong, Y. Wang and S. Xuan, *Compos. Sci. Technol.*, 2016, **135**, 92–99.

21 H. Pang, S. Xuan, T. Liu and X. Gong, *Soft Matter*, 2015, **11**, 6893–6902.

22 T. Hu, S. Xuan, L. Ding and X. Gong, *Mater. Des.*, 2018, **156**, 528–537.

23 L. Ding, S. Xuan, J. Feng and X. Gong, *Composites, Part A*, 2017, **100**, 97–105.

24 G. Yun, S. Y. Tang, S. Sun, D. Yuan, Q. Zhao, L. Deng, S. Yan, H. Du, M. D. Dickey and W. Li, *Nat. Commun.*, 2019, **10**, 1300–1309.

25 S. Wang, L. Ding, X. Fan, W. Jiang and X. Gong, *Nano Energy*, 2018, **53**, 863–870.

26 S. Wang, L. Ding, Y. Wang and X. Gong, *Nano Energy*, 2019, **59**, 434–442.

27 C. M. Cui, X. Z. Wang, Z. R. Yi, B. Yang, X. L. Wang, X. Chen, J. Q. Liu and C. S. Yang, *ACS Appl. Mater. Interfaces*, 2018, **10**, 3652–3659.

28 Z. Ren, J. Nie, J. Shao, Q. Lai, L. Wang, J. Chen, X. Chen and Z. L. Wang, *Adv. Funct. Mater.*, 2018, **28**, 1802989.

29 X. Cui, S. Cao, R. Guo, S. A. Khan, G. Xie, Z. Tian, S. Sang and H. Zhang, *Energy Sci. Eng.*, 2019, **0**, 1–9.

30 S. A. Khan, A. Ali, A. Q. Rahimoon and P. Jalalzai, *J. Nanoelectron. Optoelectron.*, 2019, **14**, 1572–1581.

31 Y. Yang, L. Lin, Y. Zhang, Q. Jing, T. C. Hou and Z. L. Wang, *ACS Nano*, 2012, **6**, 10378.

32 S. Qi, H. Guo, J. Chen, J. Fu, C. Hu, M. Yu and Z. L. Wang, *Nanoscale*, 2018, **10**, 4745–4753.

33 S. Wang, L. Gong, Z. Shang, L. Ding, G. Yin, W. Jiang, X. Gong and S. Xuan, *Adv. Funct. Mater.*, 2018, **28**, 1707538.

34 S. Wang, S. Xuan, W. Jiang, W. Jiang, L. Yan, Y. Mao, M. Liu and X. Gong, *J. Mater. Chem. A*, 2015, **3**, 19790–19800.

35 Q. Wen, Y. Wang, J. Feng and X. Gong, *Appl. Phys. Lett.*, 2018, **113**, 081902.

36 Z. W. Ren, Y. F. Ding, J. H. Nie, F. Wang, L. Xu, S. Q. Lin, X. Y. Chen and Z. L. Wang, *ACS Appl. Mater. Interfaces*, 2019, **11**, 6143–6153.

37 S. W. Chen, X. Cao, N. Wang, L. Ma, H. R. Zhu, M. Willander, Y. Jie and Z. L. Wan, *Adv. Energy Mater.*, 2017, **7**, 1601255.